AIP | Journal of Applied Physics

Defect mechanisms in the In2O3(ZnO)k system (k=3, 5, 7, 9)

E. Mitchell Hopper, Haowei Peng, Steven A. Hawks, Arthur J. Freeman, and Thomas O. Mason

Citation: J. Appl. Phys. **112**, 093712 (2012); doi: 10.1063/1.4764924
View online: http://dx.doi.org/10.1063/1.4764924
View Table of Contents: http://jap.aip.org/resource/1/JAPIAU/v112/i9
Published by the American Institute of Physics.

Defect mechanisms in the $In_2O_3(ZnO)_k$ system (k = 3, 5, 7, 9)

E. Mitchell Hopper,[1] Haowei Peng,[2] Steven A. Hawks,[1] Arthur J. Freeman,[2] and Thomas O. Mason[1]
[1]*Department of Materials Science and Engineering, Northwestern University, Evanston, Illinois 60208, USA*
[2]*Department of Physics and Astronomy, Northwestern University, Evanston, Illinois 60208, USA*

(Received 8 August 2012; accepted 12 October 2012; published online 8 November 2012)

The defect chemistry of several compounds in the $In_2O_3(ZnO)_k$ series (k = 3, 5, 7, and 9) was investigated in bulk specimens by analysis of the dependence of their conductivity on the oxygen partial pressure. The resulting Brouwer slopes were inconsistent with a doubly charged oxygen vacancy defect model, and varied with the phase. The k = 3 phase had behavior similar to donor-doped In_2O_3, and the behavior of the other phases resembled that of donor-doped ZnO. The donor in both cases is proposed to be In occupying Zn sites. First principles calculations of the formation energy of intrinsic defects in this system support the proposed models. The present work expands prior theoretical analysis to include acceptor defects, such as cation vacancies (V_{Zn}, V_{In}) and oxygen interstitials (O_i). © *2012 American Institute of Physics*. [http://dx.doi.org/10.1063/1.4764924]

INTRODUCTION

Transparent conducting oxides (TCOs) are a class of materials that possess both electrical conductivity (>1000 S/cm) and optical transparency (>80% in thin film form). This combination makes them critical components of devices like photovoltaics, flat panel displays, and light emitting diodes, where they act as transparent electrodes.[1]

The benchmark TCO is Sn-doped In_2O_3 (ITO), which has good transparency and has achieved conductivities exceeding 10 000 S/cm.[2,3] However, the scarcity of In and the increasing demand for transparent electrode materials has resulted in ITO cost volatility.[4] Additionally, the work function of ITO is generally lower than the 5 eV needed for organic photovoltaic applications,[5–7] and ITO is etched by Poly(3,4-ethylenedioxythiophene) poly(styrenesulfonate) (PEDOT:PSS), an electron blocking layer typically used in conjunction with the TCO layer in organic photovoltaics.[8–10] These shortcomings motivate a search for TCOs with lower In contents that can compete with the electrical performance of ITO.

One such system is the group of indium zinc oxide compounds with the formula $In_2O_3(ZnO)_k$, where k is an integer. These compounds possess a layered structure, consisting of alternating In-O layers and In-Zn-O layers, the latter of which increases in thickness with k. Members of this system are of interest because they have relatively high work functions compared to other TCOs (Ref. 11) and have excellent transmission across the infrared and visible spectrum.[12] Because these compounds have 50% or less In on a cation basis, they are also attractive from an economic perspective. The $In_2O_3(ZnO)_2$ and $In_2O_3(ZnO)_3$ phases exhibit markedly higher conductivity and mobility than phases with higher Zn contents (1500 S/cm for undoped thin films of the k = 2 phase[13] and 3000 S/cm with doping[14]) and are, therefore, the most thoroughly studied in the literature for photovoltaic applications. However, the phases with higher Zn content turn out to possess thermoelectric properties that rival those of the k = 2 and 3 phases, and are thus of great interest for thermoelectric power generation.[15,16] Furthermore, their layered structure contributes to an increase in the thermoelectric figure of merit, through a reduction in thermal conductivity. A more thorough investigation of the series as a whole, then, is necessary to understand the dramatic change in electrical conductivity observed among compounds in this system. In particular, the intrinsic source of defects, which lends these materials high carrier concentrations even when nominally undoped, is unclear.

In the $In_2O_3(ZnO)_k$ compounds, as in many other n-type oxides, it has often been assumed that ionized oxygen vacancies are the donor species responsible for the intrinsic n-type character.[17–20] This assumption is based primarily on the fact that the conductivity of thin films increases as the oxygen content in the deposition atmosphere is reduced. However, a simple oxygen vacancy mechanism cannot account for the large variation in carrier concentration (n) observed among $In_2O_3(ZnO)_k$ phases. For example, n has been reported to decrease by more than an order of magnitude between the k = 3 and k = 11 phases[21] in samples synthesized under identical atmospheres. Furthermore, first-principles theoretical calculations predict that oxygen vacancies should occupy deep levels in the related oxides In_2O_3,[22,23] ZnO,[22] and $InGaO(ZnO)_k$,[24] and thus cannot act as efficient donors in these systems. Recent work by the authors confirmed this for the $In_2O_3(ZnO)_3$ phase.[25] This suggests that the dominant defect mechanism in the $In_2O_3(ZnO)_k$ system depends on the crystal structure or cation composition, as well as the oxygen pressure during synthesis. Recent first-principles calculations by the authors suggested that the most likely donor defect is the In anti-site defect, which consists of an In atom occupying a Zn lattice site ($In_{Zn}^{\bullet}$).[25]

In the current work, the defect chemistry of four $In_2O_3(ZnO)_k$ phases (k = 3, 5, 7, and 9) was investigated in bulk specimens by "Brouwer analysis" of the dependence of their equilibrium electrical properties on oxygen partial pressure at intermediate temperature (750 °C). These phases were chosen because they represent a wide range of composition and electrical properties; in particular, the k = 3 phase

has the highest conductivity and mobility of any of the $In_2O_3(ZnO)_k$ phases that have been studied in bulk form.[21] To provide support for the prevalence of the defects suggested by this analysis, the formation energy calculations discussed above have been expanded to include intrinsic acceptor defects.

EXPERIMENTAL PROCEDURE

Bulk polycrystalline samples of $In_2O_3(ZnO)_k$ (k = 3, 5, 7, and 9) were fabricated by conventional solid state synthesis. Starting powders of In_2O_3 (99.99%, Alfa Aesar, Ward Hill, MA) and ZnO (99.999%, Alfa Aesar) were thoroughly mixed and pressed into pellets, which were calcined in air at 1000 °C for 12 h. To prevent contamination from the crucible wall and to limit Zn loss due to vaporization at high temperatures, pellets were surrounded by beds of sacrificial powder of the same composition and placed inside several nested crucibles. The pellets were ground and repressed following calcination, and then sintered at 1300 °C for 24 h. The k = 5, 7, and 9 pellets were cooled slowly (6 °C/min), but the k = 3 pellets were air quenched owing to the fact that the phase is unstable below 1250 °C.[21] The phase purity of the sintered pellets was confirmed by x-ray diffraction using a Rigaku diffractometer (Rigaku, Inc., Tokyo, Japan) with a Cu K_α source.

The electrical conductivities of bar-shaped samples cut by diamond saw from the sintered ceramic pellets of each compound were measured at 750 °C by four-point measurements, as described by Hong *et al.*[26] The calculated conductivities were corrected for porosity using the Bruggeman symmetric model[27] and averaged between forward and reverse current to account for the Seebeck voltage generated by the temperature difference along the length of the samples.

The variation in carrier concentration required for Brouwer analysis was achieved by letting each sample equilibrate under a range of oxygen partial pressures (pO_2). The pO_2 was varied between 21% and 0.01% (100 ppm) O_2, obtained using commercial mixtures of argon and oxygen, and confirmed by a Thermox CG 1000 oxygen analyzer (Ametek Inc., Paoli, PA). The conductivity was allowed to reach its equilibrium value for each pO_2, which typically took from several days to a week to achieve.

THEORETICAL PROCEDURE

The projector-augmented-wave method,[28] as implemented in the Vienna *ab-initio* simulation package (VASP),[29] was used for the calculation of defect formation enthalpies. The Perdew-Burke-Ernzerhof generalized gradient approximation (GGA)[30] was used to describe the exchange-correlation interaction. Zn 3*d* and In 4*d* electrons were treated as valence electrons explicitly, and the electron wave functions were expanded with plane waves up to a kinetic energy of 450 eV. A Γ-centered $2 \times 4 \times 2$ Monkhorst-Pack *k*-mesh[31] was used for Brillouin zone integration of the 66-atom $In_2O_3(ZnO)_3$ primitive unit cell, which was fully relaxed until the residual atomic forces were less than 0.01 eV/Å.

The formation energy (ΔH) of a defect D with a charge q was determined by modeling supercells with and without the defect, and defined by[32,33]

$$\Delta H_{D,q}(E_F, \mu) = E_{D,q} - E_H + \sum n_\alpha(\mu_\alpha^0 + \Delta\mu_\alpha) + q(E_V + E_F). \quad (1)$$

In this equation, $E_{D,q}$ and E_H represent the total energies of the supercell with and without the defect, respectively. The Fermi level, E_F, is defined in reference to the valence band maximum, E_V, n_α is the number of atoms of element α removed from the pristine host supercell, and $\Delta\mu_\alpha$ is the chemical potential of element α with respect to the reference energy for that element, μ_α^0. The procedure used to calculate the chemical potential of each element was previously described in detail by Peng *et al.*[25] Corrections described by Lany and Zunger[32] were applied to account for the finite size of the supercell and the band gap error characteristic of the GGA approximation. These corrections matched the calculated results to the band gap determined experimentally for the $In_2O_3(ZnO)_3$ phase, 2.72 eV.[15] Because of the prohibitively large unit cell size of phases with higher k values, calculations were limited to the $In_2O_3(ZnO)_3$ structure. However, the trends in defect formation energies are expected to be similar for the k = 5, 7, and 9 phases.

RESULTS AND DISCUSSION

Defect reactions are written in Kröger-Vink notation, which accounts for the mass, charge, and location of crystallographic defects. As an example, the oxygen vacancy defect mechanism often assumed to determine the carrier concentration in the $In_2O_3(ZnO)_k$ system involves the following reaction:

$$O_O^\times \leftrightarrow \frac{1}{2}O_2(g) + V_O^{\bullet\bullet} + 2e'. \quad (2)$$

This describes the formation of a positively charged oxygen vacancy ($V_O^{\bullet\bullet}$) and two free electrons (e') upon the removal of an oxygen ion from the lattice. The equilibrium constant (K_{eq}) for this reaction can be simplified by substituting in the electroneutrality condition ($n = 2[V_O^{\bullet\bullet}]$) as follows:

$$K_{eq} = (pO_2)^{\frac{1}{2}}[V_O^{\bullet\bullet}]n^2 = \frac{1}{2}(pO_2)^{\frac{1}{2}}n^3. \quad (3)$$

Since K_{eq} is a constant, an increase in the pO_2 must be accompanied by a decrease in the carrier concentration according to the following power law relationship:

$$n \propto (pO_2)^{-\frac{1}{6}}. \quad (4)$$

The electrical conductivity (σ) is the product of the carrier concentration (n), the electronic charge, and the mobility. Because the mobility is fairly constant over the range of carrier concentrations reported for this system,[11,21] the conductivity is directly proportional to the carrier concentration and thus has the same power law dependence on the pO_2,

$$\sigma \propto (pO_2)^{-\frac{1}{6}}. \quad (5)$$

Based on this relationship, a log-log plot of conductivity vs. pO_2 (called a Brouwer diagram) for samples equilibrated under several different oxygen partial pressures would be expected to have a slope of −1/6 if oxygen vacancies were the dominant defect.

Brouwer diagrams (log(conductivity) vs. log(pO_2)) for the k = 3, 5, 7, and 9 phases are shown in Fig. 1. All phases follow the straight lines characteristic of a power law relationship between conductivity and pO_2. As expected, the conductivity decreases monotonically with increasing Zn content (from the k = 3 to k = 9 phases) at all oxygen partial pressures. However, because the Brouwer diagram slopes are not −1/6, the oxygen vacancy mechanism described above cannot be responsible for the electronic behavior of these materials. Additionally, there are apparently two defect mechanisms at work, depending on the phase. The k = 3 phase Brouwer diagram (Fig. 1(a)) has a −1/8 slope, while the k = 5, 7, and 9 phases (Fig. 1(b)), which have lower conductivities, exhibit −1/4 slopes.

Two well-understood systems that can help explain this behavior are In_2O_3 and ZnO, the basis oxides that make up the $In_2O_3(ZnO)_k$ compounds. In phases with low values of k, the In-O layers of $In_2O_3(ZnO)_k$ materials are fairly close to one another, and the In concentration in the In-Zn-O layers is high. Given the reported contribution of the In-O layers to the electron mobility in these compounds,[13] it is plausible that for compounds with low values of k, In dominates the electronic behavior of the material.

As the value of k increases, the Zn concentration of the overall material increases as well. The structure of the In-O layers, however, remains constant, with the extra Zn incorporated by an increase in the thickness of the In-Zn-O layers and a decreasing In concentration within these layers. Thus, for high values of k, the atomic structure begins to resemble that of ZnO, and the behavior of the material as a whole is likely to be strongly influenced by that of ZnO.

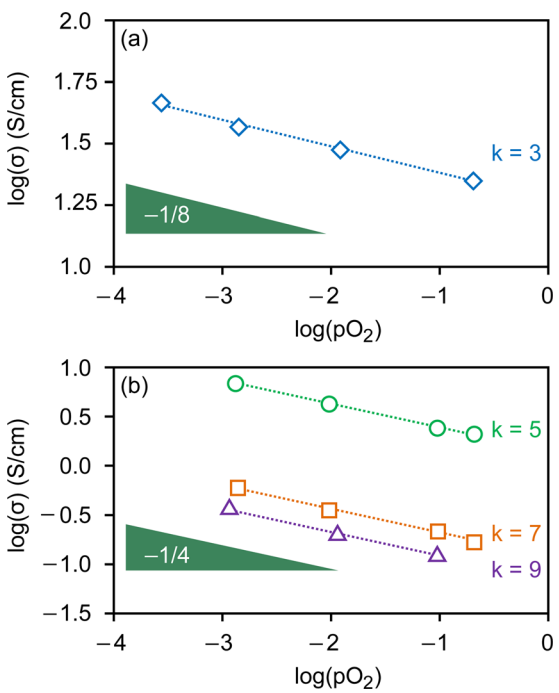

FIG. 1. Brouwer diagrams of the $In_2O_3(ZnO)_k$ series at 750 °C for (a) k = 3 (diamonds) and (b) k = 5 (circles), 7 (squares), and 9 (triangles).

Since $In_2O_3(ZnO)_k$ compounds are persistently n-type, the most relevant comparisons would be to donor-doped In_2O_3 and ZnO. The most common dopants are Sn^{4+}, which replaces In^{3+} in In_2O_3 to make ITO, and Al^{3+}, which replaces Zn^{2+} in Al-doped ZnO. Under oxidizing conditions (similar to those in the current experiment), the defect chemistry of Sn-doped In_2O_3 is dominated by a neutral associate of Sn donors and O interstitials, known as the Frank-Köstlin cluster, which can be written as $(2Sn_{In}^{\bullet}O_i'')^{\times}$.[34] The dissolution of these clusters as oxygen is removed from the material gives rise to a −1/8 slope in Brouwer plots of the conductivity vs. pO_2 (see Fig. 2(a)).[35]

The Brouwer diagram for donor doped ZnO, calculated by Lany and Zunger[22] and shown schematically in Fig. 2(b), presents markedly different behaviors from ITO. Under reducing conditions, the majority defects are Al donors, so *n* is fixed by the concentration of these donors and is independent of the pO_2. Under oxygen-rich conditions, the donors still exist but are increasingly compensated by the so-called "killer defects:" Zn vacancies that, as acceptors, tend to negate the effect of the Al donors. The ionic compensation of donors by the "electron killer" vacancies leads to a −1/4 slope for electrons on the Brouwer diagram for Al:ZnO.

The conductivity vs. pO_2 behavior of the $In_2O_3(ZnO)_k$ phases discussed above can be understood by analogy to the mechanisms dominating donor-doped In_2O_3 and ZnO. Although there are no aliovalent dopants in the samples investigated in the current work, In anti-site defects ($In_{Zn}^{\bullet}$) have recently been shown to have very low formation energies in these compounds, and are thus likely to be the dominant donor species.[25] In the $In_2O_3(ZnO)_3$ phase, this defect can explain the observed behavior by a model analogous to carrier formation in donor-doped In_2O_3,

$$(2In_{Zn}^{\bullet}O_i'')^{\times} \leftrightarrow \frac{1}{2}O_2(g) + 2In_{Zn}^{\bullet} + 2e'. \quad (6)$$

As with the oxygen vacancy mechanism described earlier, the electroneutrality condition requires that the concentration

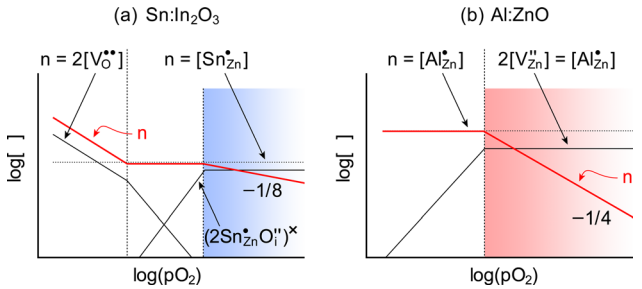

FIG. 2. Schematic Brouwer diagrams of (a) Sn:In_2O_3, showing the effect of the Frank-Köstlin cluster on the oxygen dependence of conductivity and (b) Al:ZnO, reflecting the effect of "electron killer" Zn vacancies at high pO_2. The shaded regions indicate the oxidizing pO_2 regime investigated in the current work.

of donors (In anti-site defects in this case) is balanced by that of the electrons as follows:

$$n = [\mathrm{In}_{\mathrm{Zn}}^{\bullet}]. \tag{7}$$

The equilibrium constant for this reaction is

$$K_{eq} = \frac{(\mathrm{pO_2})^{\frac{1}{2}}[\mathrm{In}_{\mathrm{Zn}}^{\bullet}]n^2}{[(2\mathrm{In}_{\mathrm{Zn}}^{\bullet}\mathrm{O}_{\mathrm{i}}'')^{\times}]}. \tag{8}$$

Substituting the electroneutrality condition into the expression for K_{eq} and assuming that the neutral associates are majority species (and therefore do not vary in concentration with pO_2) provide the Brouwer relationship that would be observed for a material dominated by this defect mechanism

$$\sigma \propto (\mathrm{pO_2})^{-\frac{1}{8}}. \tag{9}$$

This would account for the $-1/8$ power law dependence of conductivity on pO_2 observed in the $In_2O_3(ZnO)_3$ phase.

The $-1/4$ slope observed in the Brouwer plot of the more Zn-rich $k = 5$, 7, and 9 phases is the same as that observed for donor-doped ZnO. The donor $In_{Zn}^{\bullet}$ still exists in these compounds, but in lower concentrations; the dominant defect reaction is instead

$$2\mathrm{e}' + \frac{1}{2}\mathrm{O_2(g)} \leftrightarrow \mathrm{O_O^{\times}} + \mathrm{V''_{Zn}}. \tag{10}$$

The key difference between the model for these phases and that for the $In_2O_3(ZnO)_3$ phase is that whereas the donors in the $In_2O_3(ZnO)_3$ model are compensated by free electrons, in this model, the electrons are minority species and the donors are instead ionically compensated by negatively charged Zn vacancies. The electroneutrality condition in this case is then dominated by these two species

$$2[\mathrm{V}_{\mathrm{Zn}}''] = [\mathrm{In}_{\mathrm{Zn}}^{\bullet}]. \tag{11}$$

The relationship between conductivity and pO_2 is again determined by the equilibrium constant

$$K_{eq} = \frac{[\mathrm{V}_{\mathrm{Zn}}''][\mathrm{O}_{\mathrm{O}}^{\times}]}{n^2(\mathrm{pO_2})^{\frac{1}{2}}}. \tag{12}$$

Assuming that the zinc vacancy content is fixed by the In anti-site population (and therefore does not vary in concentration with pO_2) gives rise to the Brouwer exponent observed in these samples

$$\sigma \propto (\mathrm{pO_2})^{-\frac{1}{4}}. \tag{13}$$

It is important to note that a given conductivity-pO_2 relationship is not unique to a particular defect model. For this reason, it is necessary to confirm the validity of the proposed defect models through additional methods. The proposed anti-site and vacancy defects are difficult to detect with experimental techniques because of their low concentrations, so the formation energies of possible defects in the $In_2O_3(ZnO)_k$ structure have been calculated from first principles. The formation energies of donor defects in $In_2O_3(ZnO)_k$, which strongly influence their concentration, were recently investigated by the authors,[25] and it was demonstrated that the donor with the lowest formation energy is the In anti-site defect (In_{Zn}). These calculations also confirmed that O vacancies occupy deep levels within the band gap and therefore cannot be ionized, which explains why the Brouwer slopes in Fig. 1 indicate a different dominant defect mechanism. The present work expands this analysis to acceptor defects, which include cation vacancies (V_{Zn}, V_{In}) and oxygen interstitials (O_i).

The calculated formation energy of these defects at the sintering temperature as a function of the Fermi level and pO_2 is plotted in Fig. 3. Sloped lines in these plots indicate that a defect is ionized at the corresponding Fermi level, with the charge on the defect given by the magnitude of the slope. This occurs when the energy level of the defect is above the Fermi energy in the case of donors, whereas the opposite is true for acceptors. The most helpful Fermi levels to consider are those encountered in experimental samples, which have been measured in previous experiments by diffuse reflectance (2.7 eV) (Ref. 15) and ultraviolet photoelectron spectroscopy (~3.0 eV).[36] For comparison of calculations with experimental results, then, the right-hand sides of the plots in Fig. 3 are the most relevant. The following discussion considers the formation energies only at this high Fermi level, indicated by the shaded regions in each plot.

The dominant acceptor defect in the high-Zn-content phases is proposed to be the Zn vacancy, and as shown in Fig. 3, V_{Zn} has a significantly lower formation energy than other acceptors in this system. At the Fermi level of the experimental samples, V_{Zn} is fully ionized and has a formation energy very close to that of the dominant donor, $In_{Zn}^{\bullet}$. This provides strong support for the model proposed for the $k = 5$, 7, and 9 phases, which predicts comparable concentrations of In anti-site defects and Zn vacancies. Further support for the In_2O_3-like defect model proposed for the $k = 3$ phase could be obtained by calculating the formation energy of the

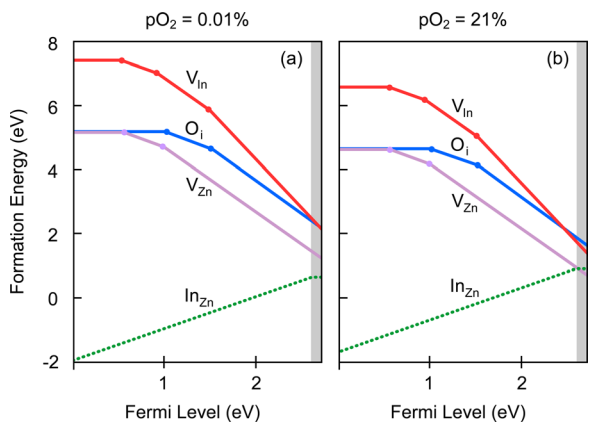

FIG. 3. Formation energies of oxygen interstitials (O_i), Zn vacancies (V_{Zn}), In vacancies (V_{In}), and In anti-site defects (In_{Zn}) as a function of Fermi level position in $In_2O_3(ZnO)_3$ at the sintering temperature (1300 °C). Sloped lines indicate an ionized defect, and horizontal lines indicate a neutral defect. Calculations were performed for oxygen concentrations of (a) 0.01% and (b) 21%. The grey region indicates the Fermi level of experimental samples.

neutral $(2In_{Zn}^{\bullet}O_i'')^{\times}$ cluster, but owing to the large number of possible configurations of this cluster within the $In_2O_3(ZnO)_3$ structure, such calculations were not attempted.

Even though the trends in defect formation energies are likely to be similar for the k = 3, 5, 7, and 9 of members of the $In_2O_3(ZnO)_k$ series, this does not mean that the relative concentrations will be the same; the defect concentrations also depend on the overall composition of the phase. This change in composition, then, is suspected to be responsible for the change in defect mechanism from the k = 3 phase to the other k = 5, 7, and 9 phases studied.

CONCLUSION

The defect mechanisms at work in the $In_2O_3(ZnO)_k$ system have been investigated by a combined experimental and theoretical approach. Brouwer analysis, which measures the dependence of a material's conductivity on the oxygen partial pressure, was carried out on bulk samples of the k = 3, 5, 7, and 9 members of the system.

It was revealed that two distinct defect mechanisms occur, depending on the phase. The compound with the highest In content available in bulk form, $In_2O_3(ZnO)_3$, has a different Brouwer slope than the more Zn-rich phases. The presence of two defect regimes is attributable to the competition between In_2O_3- and ZnO-like behavior as the crystal structure progresses from one dominated by In (k = 3) to those more similar to ZnO (k = 5, 7, and 9). The donor in both cases is proposed to be the In antisite defect, $In_{Zn}^{\bullet}$. First principles calculations of the formation energies of acceptor defects in the $In_2O_3(ZnO)_3$ structure, together with previous calculations of donor defect formation energies suggesting the prevalence of $In_{Zn}^{\bullet}$, provided support for these models by confirming that Zn vacancies, crucial to the defect mechanism proposed for the k = 5, 7, and 9 phases, have a formation energy comparable to $In_{Zn}^{\bullet}$ and significantly lower than other potential acceptors in this system.

ACKNOWLEDGMENTS

This work was supported by the U.S. Department of Energy under Grant no. DE-FG02-08ER46436 and made use of the J. B. Cohen X-ray Diffraction Facility supported by the MRSEC program of the National Science Foundation (DMR-1121262) at the Materials Research Center of Northwestern University.

[1]B. G. Lewis and D. C. Paine, MRS Bull. **25**, 22–27 (2000).
[2]I. A. Rauf, Mater. Lett. **18**, 123–127 (1993).
[3]P. Nath, R. F. Bunshah, B. M. Basol, and G. M. Staffsud, Thin Solid Films **72**, 463–468 (1980).
[4]C. A. Hoel, T. O. Mason, J. F. Gaillard, and K. R. Poeppelmeier, Chem. Mater. **22**, 3569–3579 (2010).
[5]Y. Harima, K. Yamashita, H. Ishii, and K. Seki, Thin Solid Films **366**, 237–248 (2000).
[6]B. W. D'Andrade, S. Datta, S. R. Forrest, P. Djurovich, E. Polikarpov, and M. E. Thompson, Org. Electron. **6**, 11–20 (2005).
[7]A. Klein, C. Körber, A. Wachau, F. Säuberlich, Y. Gassenbauer, S. P. Harvey, D. E. Proffit, and T. O. Mason, Materials **3**, 4892–4914 (2010).
[8]N. R. Armstrong, C. Carter, C. Donley, A. Simmonds, P. Lee, M. Brumack, B. Kippelen, B. Domercq, and S. Yoo, Thin Solid Films **445**, 342–352 (2003).
[9]J. Cui, Q. Huang, J. C. G. Veinot, H. Yan, Q. Wang, G. R. Hutchison, A. G. Richter, G. Evmenenko, P. Dutta, and T. J. Marks, Langmuir **18**, 9958–9970 (2002).
[10]J. Ni, H. Yan, A. Wang, Y. Yang, C. L. Stern, A. W. Metz, S. Jin, L. Wang, T. J. Marks, J. R. Ireland, and C. R. Kannewurf, J. Am. Chem. Soc. **127**, 5613–5624 (2005).
[11]T. Minami, MRS Bull. **25**, 38–44 (2000).
[12]J. M. Phillips, R. J. Cava, G. A. Thomas, S. A. Carter, J. Kwo, T. Siegrist, J. J. Krajewski, J. H. Marshall, W. F. Peck, and D. H. Rapkine, Appl. Phys. Lett. **67**, 2246 (1995).
[13]N. Naghavi, L. Dupont, C. Marcel, C. Maugy, A. Rougier, C. Gue, and J. M. Tarascon, Electrochim. Acta **46**, 2007–2013 (2001).
[14]T. Minami, T. Kakumu, and S. Takata, J. Vac. Sci. Technol. A **14**, 1704 (1996).
[15]E. M. Hopper, Q. Zhu, J.-H. Song, H. Peng, A. J. Freeman, and T. O. Mason, J. Appl. Phys. **109**, 013713 (2011).
[16]S. Isobe, T. Tani, Y. Masuda, W.-S. Seo, and K. Koumoto, Jpn. J. Appl. Phys., Part I **41**, 731–732 (2002).
[17]Y. Orikasa, N. Hayashi, and S. Muranaka, J. Appl. Phys. **103**, 113703 (2008).
[18]N. Naghavi, A. Rougier, C. Marcel, C. Guery, J. B. Leriche, and J.-M. M. Tarascon, Thin Solid Films **360**, 233–240 (2000).
[19]S. Hirano, S. Isobe, T. Tani, N. Kitamura, I. Matsubara, and K. Koumoto, Jpn. J. Appl. Phys., Part I **41**, 6430–6435 (2002).
[20]H. Kaga, R. Asahi, and T. Tani, Jpn. J. Appl. Phys., Part I **43**, 7133–7136 (2004).
[21]T. Moriga, D. D. Edwards, T. O. Mason, G. B. Palmer, K. R. Poeppelmeier, J. L. Schindler, and C. R. Kannewurf, J. Am. Ceram. Soc. **81**, 1310–1316 (1998).
[22]S. Lany and A. Zunger, Phys. Rev. Lett. **98**, 045501 (2007).
[23]T. Tomita, K. Yamashita, Y. Hayafuji, and H. Adachi, Appl. Phys. Lett. **87**, 051911 (2005).
[24]H. Omura, H. Kumomi, K. Nomura, T. Kamiya, M. Hirano, and H. Hosono, J. Appl. Phys. **105**, 093712 (2009).
[25]H. Peng, J.-H. Song, E. M. Hopper, Q. Zhu, T. O. Mason, and A. J. Freeman, Chem. Mater. **24**, 106–114 (2012).
[26]B.-S. Hong, S. J. Ford, and T. O. Mason, Key Eng. Mater. **125–126**, 163–186 (1997).
[27]D. S. McLachlan, M. Blaszkiewicz, and R. E. Newnham, J. Am. Ceram. Soc. **73**, 2187–2203 (1990).
[28]P. E. Blöchl, Phys. Rev. B **50**, 17953 (1994).
[29]G. Kresse and J. Hafner, Phys. Rev. B **48**, 13115 (1993).
[30]J. P. Perdew, K. Burke, and M. Ernzerhof, Phys. Rev. Lett. **77**, 3865–3868 (1996).
[31]H. J. Monkhorst and J. D. Pack, Phys. Rev. B **13**, 5188–5192 (1976).
[32]S. Lany and A. Zunger, Phys. Rev. B **78**, 235104 (2008).
[33]S.-H. Wei, Comput. Mater. Sci. **30**, 337 (2004).
[34]G. Frank and H. Kostlin, Appl. Phys. A **27**, 197–206 (1982).
[35]S. P. Harvey, T. O. Mason, Y. Gassenbauer, A. Klein, and R. Schafranek, J. Phys. D: Appl. Phys. **39**, 3959–3968 (2006).
[36]E. M. Hopper, Q. Zhu, J. Gassmann, A. Klein, and T. O. Mason, "Surface electronic properties of polycrystalline bulk and thin film $In_2O_3(ZnO)_k$ compounds," Appl. Surf. Sci. (to be published).